Surface roughness and surface-induced resistivity of gold films on mica: Application of quantitative scanning tunneling microscopy

Raúl C. Munoz,* Guillermo Vidal, Marcelo Mulsow, Judit G. Lisoni, Claudio Arenas, Andres Concha, Fernando Mora, and Roberto Espejo
Departamento de Física and Departamento de Ingeniería Eléctrica, Facultad de Ciencias Físicas y Matemáticas, Universidad de Chile, Blanco Encalada 2008, Casilla 487-3, Santiago, Chile

Germán Kremer and Luis Moraga
Departamento de Física, Facultad de Ciencias, Universidad de Chile, Las Palmeras 3425, Santiago, Chile

Rolando Esparza and Patricio Haberle
Departamento de Física, Universidad Técnica Federico Santa María, Casilla 110-V, Valparaíso, Chile
(Received 15 December 1999; revised manuscript received 30 March 2000)

We report measurements of the resistivity $\rho(T)$ of a gold film 70 nm thick deposited on mica preheated to 300 °C in UHV, performed between 4 and 300 K, and measurements of the surface topography of the same film performed with a scanning tunneling microscope (STM). From the roughness measured with the STM we determine the parameters δ (rms amplitude) and ξ (lateral correlation length) corresponding to a Gaussian representation of the average height-height autocorrelation function (ACF). We use the parameters δ and ξ to calculate the quantum reflectivity R and the increase in resistivity induced by electron-surface scattering on this film, according to a modified version of the theory of Sheng, Xing, and Wang (mSXW) [Munoz *et al.*, J. Phys.: Condens. Matter **11**, L299 (1999)]. The mSXW theory is able to select the appropriate scale of distance over which corrugations take place, leading to $R \approx 1$ for corrugations taking place over scales of distances that are long when compared to a few Fermi wavelength λ_F, and $R < 1$ for corrugations taking place over scales of distances that are comparable to λ_F (to within an order of magnitude). The reflectivity R determined by corrugations ocurring over a scale of distances comparable to λ_F approaches zero for a certain angle. The resistivity $\rho(T)$ of the film increases by roughly a factor of 4 between 4 and 300 K, and so does the bulk resistivity $\rho_0(T)$ predicted by mSXW theory. With the parameters δ and ξ measured on our 70-nm film, we reproduced approximately the thickness and temperature dependence of the resistivity (between 4 and 300 K) of several gold films on mica reported by Sambles, Elsom, and Jarvis [Philos. Trans. R. Soc. London, Ser. A **304**, 365 (1982)], *without using any adjustable parameters*. The results of this paper suggest that the relevant quantities controlling electron-surface scattering in continuous gold films of arbitrary thickness, are the parameters δ and ξ describing the average ACF that characterizes the surface of the sample on a nanoscopic scale, in agreement with the accepted view regarding the conductivity of ultrathin films.

I. INTRODUCTION

One of the fundamental problems in solid-state physics that has attracted the attention of researchers for over sixty years, relates to the effect of electron-surface scattering on the transport properties of thin metallic and semiconducting films. One of the central issues is how the surface of the structure affects its electrical transport properties, when one or more of the dimensions characterizing the structure are comparable to or smaller than the mean-free-path of the charge carriers; what is known as ''size effects.''

One of the complexities associated with size effects is related to the scale of distances involved. Arguments stemming from the wavelike nature of the electron and from wave optics have been applied to describe the collision between the electrons and the surface. These arguments point to the fact that, for the surface roughness to have an influence on the charge transport properties of the film, the scale of distances over which the surface roughness takes place and the typical amplitude of the surface roughness, should be comparable to or smaller than the characteristic wavelength of the carrier, the Fermi wavelength λ_F,[1] which for several metals is in the range of nanometers. The invention of the scanning tunneling microscope (STM) has opened the possibility of directly measuring surface roughness within the scale set by λ_F.

There is experimental evidence supporting the argument outlined above. Schumacher performed a series of carefully controlled experiments, evaporating silver onto glass slides held at 225 K under UHV; the films were annealed at 350 K after evaporation to achieve minimum resistance. A varying amount of silver atoms was further evaporated at low temperatures ($T \leqslant 100$ K) onto the annealed films and the resistivity of the films was observed to increase by a few percent with the addition of less than a monolayer.[2] However, direct evidence reporting the resistivity and the surface roughness *measured on the scale set by* λ_F *on the same film* appears to be missing.

The theoretical work concerning size effects focused for many decades on the Fuchs-Sondheimer (FS) theory. FS describe the motion of electrons in the metal film by a Boltzmann transport equation (BTE), where the effect of the

rough surface is incorporated into the boundary conditions that must be satisfied by the electron distribution function via a specularity parameter R, which represents the fraction of electrons $0 \leqslant R \leqslant 1$ that are specularly reflected upon colliding with the rough surface.[1,3]

It is well known that this approach is inadequate for very thin, high-purity samples where the film thickness t is much smaller than the bulk mean-free-path l. On the one hand, for ultrathin high-purity films, the conductivity of the film is known to exhibit a stepwise increase with increasing film thickness, as a consequence of the quantization of the electronic energy levels induced by confinement of the electron gas between two parallel potential barriers; what is known as quantum size effects (QSE). The modeling of electron motion via a BTE with FS boundary conditions, does not account for QSE. On the other hand, in the limit $l \rightarrow \infty$, the FS conductivity diverges as $\ln(l/t)$, implying that when the conductivity of the film is limited only by electron-surface scattering, there is no dissipation, an unphysical result that arises from the omission of quantum effects in the classical theory. To overcome these shortcomings, a number of quantum transport theories applicable to several special cases have been published.[4–8] The quantum transport theories succeeded in describing the experimental data in ultrathin films of $CoSi_2$.[9]

The goal of theoretical research on size effects has been to build a formalism that would permit the prediction of both the reflectivity R characterizing electron-surface scattering and the increase in resistivity due to size effects from first principles, from the information contained in the surface roughness profile. A significant step towards this goal is the theory of Sheng, Xing, and Wang (SXW), that unifies the available quantum transport theories applicable to the different special cases with the classical FS formalism.[3,10] SXW abandoned the model in which the motion of electrons in the metal film is described via BTE. They calculated instead the Green's function describing electrons confined within two potential barriers, one of which is flat, the other is a randomly rough surface. SXW computed the dissipative part of the electron self-energy due to electron-surface scattering in the presence of the rough surface using Dyson's equation, and proceeded to calculate the conductivity of the film using the Kubo transport formalism. However, in their treatment, SXW modeled the surface roughness by a white-noise surface profile, assuming that the Fourier transform of the height-height autocorrelation function (ACF) which on average characterizes the surface, is a constant independent of the in-plane momentum.[10] This white-noise approximation severely limits the predictive power of the SXW formalism.

We have recently proposed a modified version of SXW theory (mSXW) that permits the calculation of both the reflectivity R and the increase in resistivity attributable to electron-surface scattering, in films in which the average ACF is described either by a Gaussian or by an exponential.[11] The mSXW theory permits the calculation of the reflectivity R and of the ratio of film conductivity σ to bulk conductivity σ_0 attributable to electron-surface scattering, in terms of the parameters δ (the rms amplitude of the ACF) and ξ (the lateral correlation length of the ACF) on a nanoscopic scale for either of the two models, Gaussian or exponential, in a continuous film of thickness t.[11]

The experimental work related to size effects in thin metal films, during several decades, relied on the method of: (i) preparing families of samples of the same material but of different thickness under similar conditions of evaporation; (ii) measuring one or more of the transport properties of the different members of the family, most commonly the resistivity; (iii) fitting the theoretical models to the thickness and/or the temperature dependence of the data and adjusting the parameters provided by theory (specularity parameter R, bulk conductivity σ_0, and in some cases the rms roughness amplitude δ).

The data analysis often proceeds from the assumption that the specularity parameter R characterizing a family of samples of the same material prepared under similar conditions of evaporation is the same, independent of the film thickness, and is a constant independent of the momentum of the electron. The lack of direct measurements of δ and ξ in an independent experiment so far has prevented a *verification of whether or not the parameters characterizing the surface roughness inferred from fitting the resistivity data on families of thin metal films prepared under similar conditions of evaporation, actually do correspond to the surface roughness measured on these films*. The availability of a theory that permits the calculation of size effects from first principles, from the parameters δ and ξ that describe the surface profile, together with the invention of the STM that makes possible the direct measurement of δ and ξ on a nanometric scale, permits a reversal of the trend based on parameter fitting of resistivity data *without independent verification* that has dominated experimental research on size effects for decades.

This paper reports on the application of the mSXW theory, and illustrates how measurements of the roughness of the surface of the sample can be used to calculate the resistivity of the film induced by electron-surface scattering. We report measurements of the temperature dependent resistivity $\rho(T)$ of a gold film 70 nm thick deposited on mica preheated to 300 °C in UHV, performed between 4 and 300 K, and measurements of the surface topography of the *same* film performed with a STM. From the roughness measured with the STM we determine the parameters δ and ξ corresponding to a Gaussian representation of the average ACF. We use the parameters δ and ξ to calculate the reflectivity R and the bulk resistivity $\rho_0(T)$ according to mSXW theory. We chose to analyze the surface roughness data using a Gaussian rather than an exponential representation of the ACF, because modifications have been proposed to the FS theory where a Gaussian representation of the surface roughness has been employed. In this paper we compare the predictions of different versions of the classical theories with the predictions of mSXW theory using a Gaussian representation of the ACF, with the parameters δ and ξ *measured in an independent experiment*. Such comparisons will reveal interesting differences between mSXW theory and other theories.

This paper is organized as follows: In Sec. II we present a brief outline of mSXW theory. In Sec. III we present experimental details concerning the sample preparation and the measurements. In Sec. IV we present the results of this paper: the structure of the films, the average ACF's that characterize the surface of the film in different scales of length, and the reflectivity R predicted by mSXW theory for each of

the different scales of length for a Gaussian representation of the ACF. We present as well the film resistivity $\rho(T)$ measured between 4 and 300 K on this film, and the corresponding bulk resistivity $\rho_0(T)$ predicted by mSXW theory. In Sec. V we discuss these results and in Sec. VI we present a summary of this paper.

II. THEORY

The mSXW theory provides a way of calculating both the specularity function R and the increase in resistivity attributable to electron-surface scattering from first principles, using information contained in the roughness profile, if the ACF characterizing the surface of the sample is described either by a Gaussian or by an exponential. Summarizing results already published, the SXW theory leads to a quantum reformulation of the FS model, that includes the effects of electron-surface scattering via a reflectivity parameter R that can be calculated from

$$R(k_\parallel)=\left(\frac{1-k_z Q(k_\parallel)}{1+k_z Q(k_\parallel)}\right)^2, \tag{1}$$

which is Eq. (7) in Ref. 10, where $Q(k_\parallel)$ represents the dissipative part of the self-energy of the electron gas due to electron-surface scattering; with $k_z^2=k_F^2-k_\parallel^2$, where k_F stands for the Fermi momentum and $k_\parallel=(k_x,k_y)$ represents the in-plane momentum. The ratio of the film conductivity σ to bulk conductivity σ_0 may be computed in terms of the reflectivity R

$$1-\frac{\sigma}{\sigma_0}=\frac{3}{2}\frac{l}{t}\frac{1}{X_0 N_c}\sum_{n=1}^{N_c} u_n(1-u_n^2) \times\frac{[1-R(u_n)][1-E_d(u_n)]}{1-R(u_n)E_d(u_n)}, \tag{2}$$

where t is the film thickness, l the carrier mean-free-path in the bulk—*σ_0 and l represent the conductivity and mean-free-path that would be observed in a film having the same concentration of impurities as the thin film, but thick enough such that the effect of electron-surface scattering can be neglected*—

$$u_n=\frac{q_n}{k_F}=\cos\theta_n=\frac{n\pi}{tk_F},\quad X_c=\frac{tk_F}{\pi},\quad N_c=\mathrm{int}(X_c),$$

where $\mathrm{int}(M)$ stands for the integer part of M,

$$X_0=\frac{3}{2}\left[1-\frac{1}{3}\left(\frac{N_c}{X_c}\right)^2\left(1+\frac{1}{N_c}\right)\left(1+\frac{1}{2N_c}\right)\right]$$

and $E_d(u_n)=\exp[-t/(u_n l)]$, which corresponds to Eq. (11) of Ref. 10. The calculation of the electron self-energy $Q(k_\parallel)$ for the case in which the ACF is described by a Gaussian $f(x,y)=\delta^2\exp[-(x^2+y^2)/\xi^2]$ has been published.[11]

The parameters δ and ξ are determined from the height-height surface ACF $f(r_\parallel)$ defined by

$$f(r_\parallel)=S^{-1}\int_S h(a_\parallel)h(a_\parallel+r_\parallel)d^2a_\parallel, \tag{3}$$

where S denotes the surface of the sample, $r_\parallel=(x,y)$ stands for the in-plane coordinates, and $h(a_\parallel)$ represents the random height characterizing the surface roughness with respect to the average surface at $z=t$. The quantity measured with the STM is the function $h(a_\parallel)$.

Notice that in the mSXW theory, *R and σ_0 are no longer adjustable parameters*. The availability of a theory that permits the calculation of σ/σ_0 from the knowledge of the parameters (δ,ξ) that can be independently measured with the STM, suggests the traditional method of fitting parameters to the conductivity data of a family of samples of different thickness—prepared under similar conditions of evaporation—should be abandoned. *A new method to compare theory and experiment is required*. Knowing (δ,ξ) we may use Eq. (2) to compute the film conductivity σ. However, a difficulty arises because to perform this calculation, we need to know the σ_0 and l that characterize the bulk, *which, therefore, are not known apriori*. Nevertheless, using the mSXW theory, the parameters σ_0 and l can be determined by means of an iterative process that has already been published,[12] that proceeds as follows:

As a first approximation, $l(T)$ corresponding to each temperature, can be calculated from $l_1(T)=\sigma(T)mv_F/(nq^2)$, where $\sigma(T)$ is the conductivity of the film measured at temperature T, m is the electron mass, v_F is the Fermi velocity, n the electron density, and q the electron charge. This value is used to compute a first estimation of $[\sigma(T)/\sigma_0(T)]_1$, using Eq. (2), $l=l_1$, and employing the parameters δ and ξ determined from the STM measurements. A corrected value for l can then be computed from $l_2=l_1[\sigma_0(T)/\sigma(T)]_1$, and a new value of $[\sigma(T)/\sigma_0(T)]_2$ can be calculated using $l=l_2$ and Eq. (2). This process is repeated until the values of $[\sigma(T)/\sigma_0(T)]_j$ and $[\sigma(T)/\sigma_0(T)]_{j+1}$ between two successive iterations j and $j+1$ do not differ by more than 0.01%. We found that 5 to 15 iterations are sufficient to satisfy this criterion, depending on temperature and on the purity of the film.

If grain boundary scattering is negligible compared to electron-surface scattering, if electron-surface scattering taking place at the lower surface of the film (in contact with the substrate) is negligible compared to electron-surface scattering taking place at the upper (exposed) surface of the film, and if the resistivity arising from electron-impurity scattering at 300 K is small compared to that arising from electron-phonon scattering at the same temperature, then the temperature dependent bulk resistivity $\rho_0(T)=1/\sigma_0(T)$ computed through this iteration process should agree with that expected from electron-phonon scattering in crystalline gold. If the parameters (δ,ξ) chosen to describe the roughness of the surface and if the theory chosen to describe electron-surface scattering are correct, then the temperature dependence of $\rho_0(T)$ determined according to this iteration process should be consistent with a Block-Gruneisen description as recommended by Matula, using the constants A, B, C, and θ appropriate for crystalline gold:[13]

$$\rho_0(T)=\rho_R+A\left(1+\frac{BT}{\theta-CT}\right)\phi\left(\frac{\theta-CT}{T}\right),\ \text{with}$$

$$\phi(x)=4x^{-5}\int_0^x\frac{z^5\exp(z)}{[\exp(z)-1]^2}dz, \tag{4}$$

where ρ_R stands for the temperature-independent residual resistivity (attributed to impurity scattering) determined by the thin film resistivity $\rho(4.2)$ measured at 4.2 K and by the ratio $\rho_0(4.2)/\rho(4.2)$ predicted by theory.

III. EXPERIMENT

We performed some preparatory experiments to select the conditions of evaporation. The temperature of the substrate, 300 °C, the speed of evaporation, 6 nm/min, and the thickness of the film, 70 nm, were chosen such as to produce a continuous film where the influence of grain-boundary scattering would be minimized, for grain boundary scattering could influence the resistivity of the film but is *not included in the SXW theory*. A necessary condition that might help minimizing grain-boundary scattering, is that the lateral dimension D characterizing the grains that make up the samples should be at least one order of magnitude larger than the thickness t of the films for then the electrons are expected to undergo an average of several collisions with the upper/lower surface of the film before colliding with the boundary of a grain. If the thickness of the films whose resistivity is to be analyzed, is in the range of 100 nm, then the samples should be made up of grains having D of the order of several hundred nm.

The gold films were prepared by thermal evaporation of 2-mm diameter, 99.99% pure gold wire (MATKEMI) from a W basket onto $20\,\text{mm}\times 10\,\text{mm}\times 0.15\,\text{mm}$ Muscovite Ruby mica slides (GOODFELLOW). The mica was freshly cleaved before evaporation. The stainless-steel evaporator was baked for many hours after loading the mica and the gold wire until reaching a pressure in the range of 10^{-10} mbar. The thickness of the gold films was monitored during evaporation with a quartz-crystal oscillator that was calibrated with a profilometer (TENCOR). To avoid scratching the surface, the thickness was measured with the profilometer *after* the surface roughness and the resistivity of the samples had been measured. During evaporation the pressure was in the range of 10^{-9} mbar.

During the preparatory experiments designed to select the conditions of evaporation, the morphology of the samples was examined using x-ray diffraction; the crystalographic structure of the films and of the mica was determined using a Siemens D-5000 x-ray difractometer. The samples were also examined using a scanning electron microscope (SEM). The samples were kept under moderate vacuum in a dessicator between the different experimental steps (measurements of the roughness with the STM, x-ray measurements, SEM measurements, resistivity measurements, determination of the thickness with the profilometer).

The surface topography was measured with the STM running in air in the constant-current mode using W tips. STM measurements were performed with a commercial OMICRON instrument, using tungsten tips 0.25 mm in diameter and freshly etched in a 0.8 M NaOH solution. All images had 256×256 pixels. We verified that the images did not depend on the gap voltage nor on the tunneling current. Before imaging the gold samples, we verified that the freshly prepared W tips produced neat images of C atoms running on highly oriented pyrolytic graphite (HOPG). Tips that did not produce neat images of C atoms on HOPG were discarded.

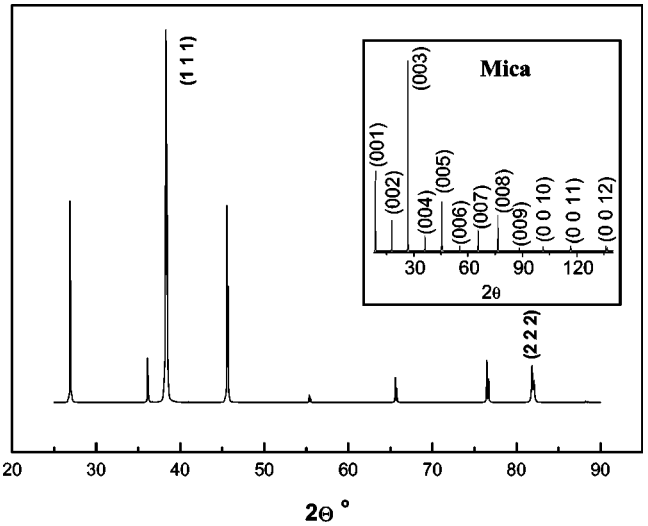

FIG. 1. θ-2θ spectra of a gold film 65 nm thick deposited on muscovite ruby mica, under UHV. The substrate was preheated to 300 °C prior to deposition, evaporation rate was 6 nm/min. The Au film was characterized using crystallographic data card JCPDS-ICDD No. 4-784. The inset shows the θ-2θ spectra of the mica substrate before evaporation of the gold film.

We paid particular attention to searching with the STM for direct experimental evidence of barriers existing between adjacent grains. For this purpose we imaged with the STM the valleys that are left after the grains coalesced to form the film. The bottom of these valleys look fairly smooth within an atomic scale. We did not find any sharp changes in the STM signal recorded on these valleys on an atomic scale, that might indicate the presence of a barrier between adjacent grains.

Conductivity measurements were performed using the four-probe method, running a current of 100 μA pp at 160 Hz, using SRS 830 lock-in amplifiers from Stanford Research. Data acquisition was computed controlled; the voltage drop across the sample was averaged over 100 data points, the relative error in the voltage readings is estimated at 2 parts in 10 000. The sample was mounted on a Cu block located in the variable temperature insert of the dewar of a 9 T (JANIS) superconducting magnet. The temperature of the Cu block was maintained within ± 0.1 K between 4 and 300 K.

The crystalographic structure of the films and the mica was determined using a Siemens D-5000 x-ray difractometer.

IV. RESULTS

A. Structure of the films

The θ-2θ spectrum is shown in Fig. 1 for a gold film 65 nm thick deposited on a mica substrate preheated to 300 °C. The rocking curve spectrum corresponding to the (111) reflection peak of Au is shown in Fig. 2. In this case both detector and source moved together during the scan and locked in a position initially fixed at an angle $2\theta = 38.314°$ corresponding to the (111) peak of gold. The radiation used was the $K\alpha$ line of Cu, with a wavelength $\lambda_\alpha = 0.154$ nm. The full width at half maximum (FWHM) of the gold (111) peak is about 0.9°.

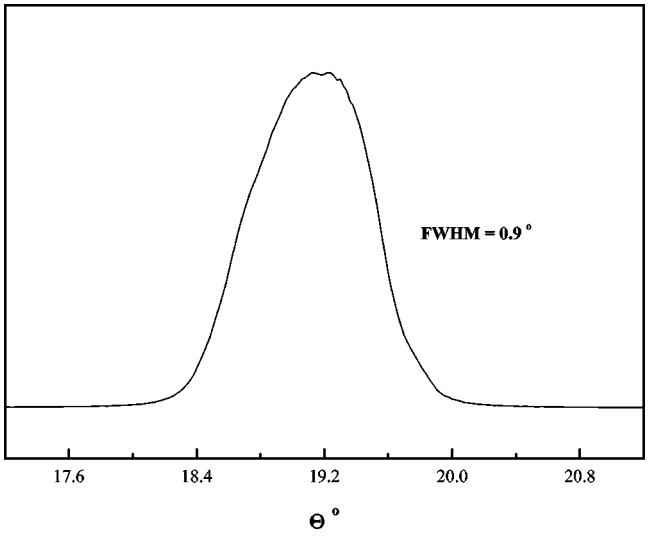

FIG. 2. Rocking-curve spectrum corresponding to the peak Au(111).

The results shown in Figs. 1 and 2 contain some interesting information: (i) The mica substrate is crystaline, and of excellent quality, since we can detect reflection peaks up to the 12th order (0012); (ii) The gold film grew along direction (111) with its surface oriented perpendicular to direction (001) of the mica; (iii) The crystalites that make up the gold film may exhibit orientational azimuthal disorder along the normal to the surface. However, any disorder other than azimuthal disorder would destroy the local translational symmetry within each grain, and therefore would introduce disorder in the reciprocal lattice associated to each grain. The effect of disorder in the reciprocal lattice is to broaden and flatten the (111) peak, such that the rocking-curve peak would exhibit a FWHM considerably larger than 0.9°; (iv) The narrowness of the rocking-curve peak (Fig. 2) indicates a very small angular misalignment $\Delta\theta$ of the (111) direction of these crystalites with respect to the (001) direction normal to the mica substrate, leading to $\Delta\theta = \pm 0.45°$; (v) The position of the Au (111) peak is $2\theta = 38.314°$, which corresponds to a lattice constant $d = 0.235$ nm; (vi) The width $\Delta\theta$ of the rocking-curve peak, and the position $2\theta = 38.314°$ can be used to obtain a rough lower-limit estimation of the lateral dimension D that characterizes the crystalites that coalesced to form the film, using the Scherrer equation, $D = 0.89\lambda/(\Delta\theta \cos\theta)$ [Eq. (4.3) in Ref. 14]. The result $D \approx 18$ nm is about one order of magnitude smaller than the typical lateral dimension D of several hundred nm determined on these films from SEM images during the preparatory experiments (the SEM images we obtained were quite similar to images already published [Fig. 1(c) from Ref. 15]). This suggests that the narrowness of the rocking curve peak $\Delta\theta = \pm 0.45°$ is limited by instrumental resolution of the x-ray detector rather than by the lateral dimension D characterizing the grains. A dimension D of several hundred nm is about one order of magnitude larger than the film thickness $t = 70$ nm. Therefore, the condition necessary to minimize grain-boundary scattering (Sec. III) is satisfied.

A direct consequence of the crystaline, excellent quality of the mica substrate and the fact that the gold grew oriented along (111) perpendicular to the surface of the mica, is that the roughness at the gold-mica interface, consists essentially of cleavage steps. As already published, these cleavage steps occur rather infrequently over the scale of distance of the order of a few tens to a few hundred nm probed by the electrons. Consequently, electron-surface scattering at the gold-mica interface can be safely ignored.[11]

B. STM images and autocorrelation functions

In order to explore different scales of length, we recorded images with the STM under different experimental conditions. Since the instrument exhibits a range of in-plane (x, y) motion that spans over three orders of magnitude (from a few tenths of nm to 1 μm), it is evident that images recorded at a particular scale are likely to miss some of the details of the roughness that might occur over a scale of distances that is either one order of magnitude larger or one order of magnitude smaller than the scale chosen for scanning, unless a very large number of pixels per line is recorded. However, recording a large number of pixels of a surface that is not atomically flat, running in the constant current mode, requires a scanning time of many minutes due to limitations on speed imposed by the natural resonant frequencies of the piezoelectric scanner. A scanning time of many minutes makes the images recorded sensitive to low-frequency noise and to thermal drift in the scanner, systematic errors which are rather difficult to assess, thereby rendering questionable the large-distance information captured within the image. In order to avoid this difficulty, rather than recording an image composed of many pixels, we chose to record images made of 256×256 pixels, and to change the scale of distance to measure the surface roughness on different scales of length on different sectors of the sample chosen at random.

To discard possible artifacts, we verified that the features captured in these images were reproducible over several runs performed with the tip positioned on the same place at the beginning of each scan and using the same scanning parameters. We also verified that the image recorded while scanning forwards was consistent with the image recorded while scanning backwards; images that did not satisfy this consistency criteria were discarded. The details captured on the 20 nm$\times$20 nm scale might include the effect of the radius of curvature of the tip, for the image obtained is expected to be the convolution of the surface profile of the film with the finite radius of curvature of the tip. No attempt was made to deconvolute the radius of the tip from the images.

The average ACF that characterizes the surface of a gold film 70 nm thick on a scale of 10 nm$\times$10 nm, is shown in Fig. 3(a). It was computed as the average of 20 ACF's calculated according to Eq. (3), from the surface roughness profiles recorded at random locations of the sample on a scale of 20 nm$\times$20 nm using periodic boundary conditions,[16] from 20 images recorded with the STM containing 256×256 pixels each. The peak at the origin is 0.353 nm;[2] the observed width of the peak at FWHM is about 2 pixels.

We verified that the autocorrelations calculated using periodic boundary conditions are consistent with the autocorrelations calculated using a window of 128×128 pixels and displacing this window over the entire frame of 256×256 pixels when calculating the surface integral [Eq. (3)].

The data representing the peak at the origin of the average ACF displayed in the inset of Fig. 3(a) was fitted using the

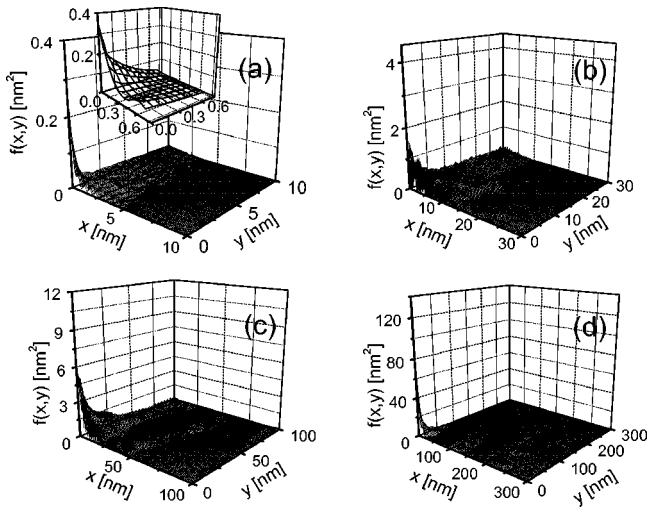

FIG. 3. (a) Average of 20 ACF's calculated from the surface roughness profiles recorded at random locations of the sample on a scale of 20 nm×20 nm using periodic boundary conditions, from 20 images recorded with the STM containing 256×256 pixels each. (x, y) represent the fast and slow scan directions, respectively. The inset shows the details of the 10×10 pixels that constitute the central peak of the average ACF. (b) Average of 25 ACF's calculated from the surface roughness profiles recorded at random locations of the sample on a scale of 60 nm×60 nm using periodic boundary conditions, from 25 images recorded with the STM containing 256×256 pixels each. (c) Average of 24 ACF's calculated from the surface roughness profiles recorded at random locations of the sample on a scale of 200 nm×200 nm using periodic boundary conditions, from 24 images recorded with the STM containing 256 ×256 pixels each. (d) Average of 29 ACF's calculated from the surface roughness profiles recorded at random locations of the sample on a scale of 600 nm×600 nm using periodic boundary conditions, from 29 images recorded with the STM containing 256 ×256 pixels each.

Gaussian $f(x,y)=\delta^2\exp[-(x^2+y^2)/\xi^2]$, employing a least-square fit procedure. When the Gaussian was fitted to the 8 ×8, 10×10, and 12×12 pixels near the origin, the values obtained were [$\delta=0.494$ nm, $\xi=0.401$ nm], [$\delta=0.448$ nm, $\xi=0.489$ nm], [$\delta=0.422$ nm, $\xi=0.549$ nm]. The corresponding values of χ^2 are 2.21, 3.78, and 7.81, respectively, indicating that the Gaussian describes well the experimental average ACF. The values obtained for ξ and δ are consistent with the atomic resolution exhibited by the tip of the STM when running on HOPG prior to measuring the gold sample; consequently the rounding-off that could be expected on the images recorded with the STM due to the finite radius of curvature of the tip, does not seem to play a significant role.

The average ACF that characterizes the surface of the sample on a scale of 30 nm×30 nm is shown in Fig. 3(b). It was computed as the average of 24 ACF's calculated from the surface roughness profiles recorded at random locations of the sample on a scale of 60 nm×60 nm using periodic boundary conditions, from 25 images recorded with the STM containing 256×256 pixels each. The peak at the origin is 4.00 nm^2 corresponding to a rms amplitude $\delta=2.00$ nm; the observed width of the peak at FWHM is less than 1 pixel.

The average ACF that characterizes the surface of the sample on a scale of 100 nm×100 nm, is shown in Fig. 3(c). It was computed as the average of 24 ACF's calculated from the surface roughness profiles recorded at random locations of the sample on a scale of 200 nm×200 nm using periodic boundary conditions, from 24 images recorded with the STM containing 256×256 pixels each. The peak at the origin is 11.5 nm^2 corresponding to a rms amplitude $\delta=3.40$ nm; the observed width of the peak at FWHM is much less than 1 pixel.

The average ACF that characterizes the surface of the gold film on a scale of 300 nm×300 nm, is shown in Fig. 3(d). It was computed as the average of 29 ACF's calculated from the surface roughness profiles recorded at random locations of the sample on a scale of 600 nm×600 nm using periodic boundary conditions, from 29 images recorded with the STM containing 256×256 pixels each. The peak at the origin is 137 nm^2 corresponding to a rms amplitude $\delta=11.7$ nm; the observed width of the peak at FWHM is much less than 1 pixel.

The interesting result displayed in Figs. 3(a)–3(d) is that, although the individual ACF's computed from each of the images recorded with the STM at random locations of the sample, at each scale of length, may differ by as much as one order of magnitude or more, and may exhibit quite different structures such as bumps and undulations away from the origin along x (fast scan direction) or along y (slow scan direction), the features away from the origin add out to nearly zero upon averaging the ACF's corresponding to each of the images, leaving essentially a sharp peak at the origin plus some noise. The width of the central peak that represents the average ACF could only be resolved when measuring the roughness of the surface on the scale of 20 nm×20 nm.

C. Surface reflectivity

The reflectivity R arising from the roughness measured in the scale of 20 nm×20 nm predicted by the mSXW formalism is shown in Fig. 4(a), calculated using ($\delta=0.455$ nm, $\xi=0.480$ nm), the average of the values for δ and ξ obtained by least-square fitting the peak at the origin of Fig. 3(a). The interesting result displayed in Fig. 4(a), is that the reflectivity predicted by the quantum theory approaches zero for a certain angle.

To calculate the reflectivity R arising from the roughness measured in the other scales, we used a Gaussian representation of the ACF, with $\xi=0.480$ nm for all scales, but $\delta=2.00$ nm for the scale of 30 nm×30 nm, $\delta=3.40$ nm for the scale of 100 nm×100 nm and $\delta=11.7$ nm for the scale of 300 nm×300 nm. The results are shown in Figs. 4(b)–4(d), respectively. The interesting and new result displayed in these figures, is that the angular dependence of the reflectivity changes drastically as the scale of distance (over which the surface roughness is measured) increases, in a way such that the larger the scale of distance, the more the reflectivity R approaches unity.

D. Resistivity

The resistivity of the 70 nm thick gold film measured as a function of temperature corrected for thermal contraction, is displayed in Fig. 5. The resistivity increases roughly by a factor of 4 when the sample is heated from 4 to 300 K.

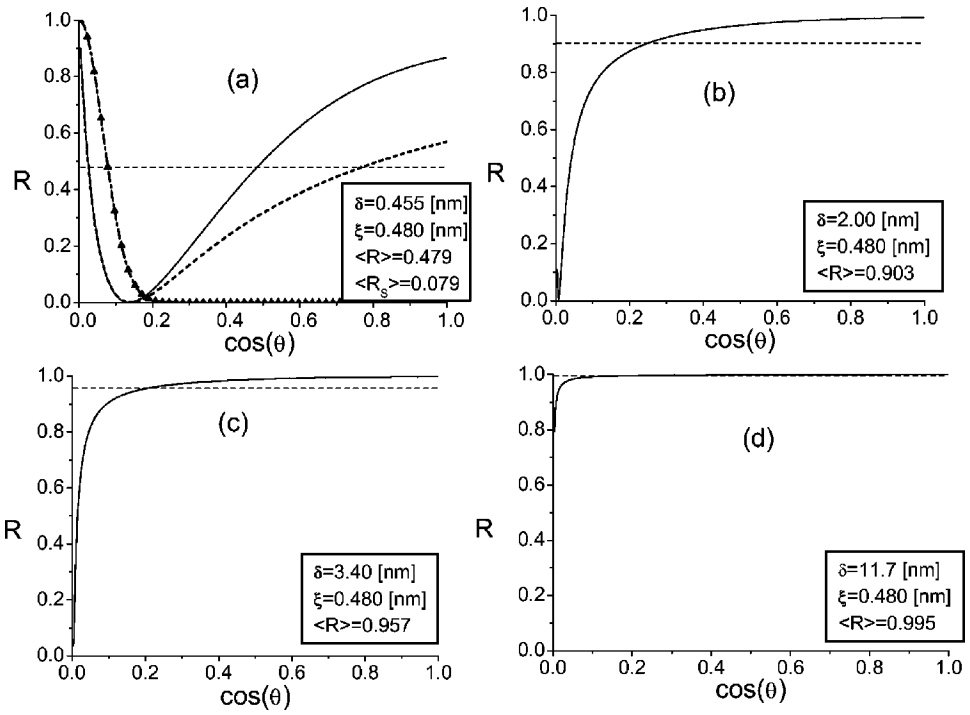

FIG. 4. (a) Reflectivity R characterizing electron-surface scattering predicted by the mSXW theory, for a film where the average ACF is described by $f(x,y)=\delta^2\exp[-(x^2+y^2)/\xi^2]$, with $\delta=0.455$ nm, $\xi=0.480$ nm, plotted as a function of $\cos(\theta)$, where θ represents the angle of incidence between the momentum of the incoming electron and the normal to the surface. The dotted line represents the white-noise reflectivity $R[f_0,\cos(\theta)]=\{[1-f_0\cos(\theta)]/[1+f_0\cos(\theta)]\}^2$ for $f_0=7.16$. The horizontal dotted line represents the average reflectivity $\langle R\rangle=0.479$ predicted by the mSXW model. The triangles-dotted line represents Soffer's reflectivity R_S [Eq. (5)]. (b) Reflectivity R characterizing electron-surface scattering predicted by mSXW theory, for a film where the average ACF is described by $f(x,y)=\delta^2\exp[-(x^2+y^2)/\xi^2]$, with $\delta=2.00$ nm, $\xi=0.480$ nm, plotted as a function of $\cos(\theta)$. The horizontal-dotted line represents the average reflectivity $\langle R\rangle=0.903$. (c) Reflectivity R characterizing electron-surface scattering predicted by mSXW theory, for a film where the average ACF is described by $f(x,y)=\delta^2\exp[-(x^2+y^2)/\xi^2]$, with $\delta=3.40$ nm, $\xi=0.480$ nm, plotted as a function of $\cos(\theta)$. The horizontal-dotted line represents the average reflectivity $\langle R\rangle=0.957$. (d) Reflectivity R characterizing electron-surface scattering predicted by the mSXW theory, for a film where the average ACF is described by $f(x,y)=\delta^2\exp[-(x^2+y^2)/\xi^2]$, with $\delta=11.7$ nm, $\xi=0.480$ nm, plotted as a function of $\cos(\theta)$. The horizontal-dotted line represents the average reflectivity $\langle R\rangle=0.995$.

V. DISCUSSION

A. Average autocorrelation function

Although the electrons are scattered by the individual corrugations they find when approaching the rough surface, in the theoretical treatment of electron-surface scattering, usually an average is performed over all corrugations found in the rough surface, such that the final answer depends on some average property of the surface, rather than on the individual corrugations. The *average corrugations* of a randomly rough surface are often assumed to exhibit certain symmetry that the individual corrugations do not necessarily possess. In quantum theories of electron-surface scattering, the *average* ACF is often assumed to be isotropic.[4–6,8,10,17,18] This means that, if $f(x,y)$ denotes the ACF defined by Eq. (3), it is expected that after averaging over the surface profile, $f(x,y)=f(\sqrt{x^2+y^2})$. Nevertheless, as pointed out in Sec. IV B, the autocorrelations computed from individual images recorded on this film certainly *do not satisfy this property*. It takes a number of the order of 20 images (or larger) recorded at *random* locations of the sample, to obtain an *average ACF that is very nearly isotropic*.

B. Amplitude of the roughness and scale of distances

An interesting prediction of the mSXW formalism concerns the scale of distances over which corrugations take place, and their relative contributions to size effects. As illustrated in Figs. 3(a)–3(d) and Figs. 4(a)–4(d), the corrugations that determine a specularity R, significantly smaller than unity, are those taking place over a scale of distances that is large compared with atomic diameter, but small compared with a mesoscopic scale; a scale of distances comparable to λ_F (in gold, $\lambda_F=0.52$ nm) to within one order of magnitude. Electrons colliding with corrugations that take place over mesoscopic scales of distances (tens of nm) or larger have only a minor influence on size effects in gold films. Electrons colliding with such corrugations undergo nearly specular scattering.

The results presented indicate that the mSXW theory is able to select the scale of distance over which corrugations take place, leading to $R\approx 1$ for corrugations taking place over scales of distances that are long when compared to a few λ_F, and $R<1$ for corrugations taking place over scales of distances that are comparable to λ_F (to within an order of magnitude). The ability of the theory to select the corrugations that take place over a scale of distances that is comparable to λ_F, as the corrugations that actually do contribute to size effects (in the sense that they lead to $R<1$), is determined by the height-height ACF. As illustrated by Figs. 3(a)–3(d) and Figs. 4(a)–4(d), when the amplitude δ grows larger than the wavelength of the carrier λ_F, the reflectivity R increases with increasing δ and it rapidly approaches unity.

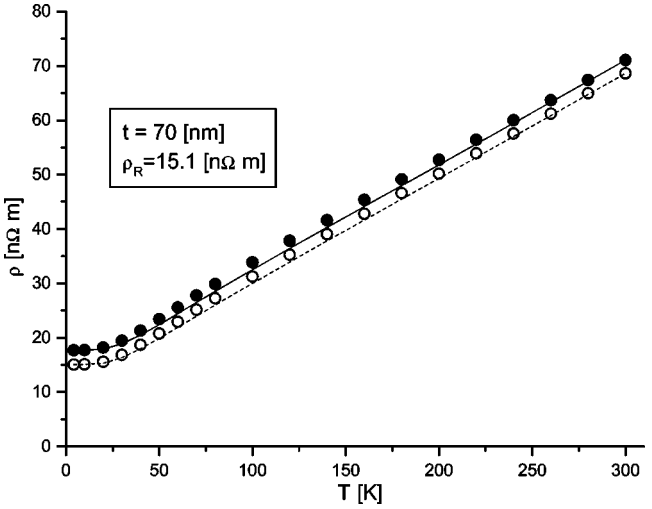

FIG. 5. Resistivity plotted as a function of temperature. Dots: resistivity measured on a 70 nm thick gold film, corrected for thermal contraction. White dots: bulk resistivity corresponding to the 70-nm gold film, calculated using mSXW theory and an ACF described by $f(x,y)=\delta^2\exp[-(x^2+y^2)/\xi^2]$, with $\delta=0.455$ nm, $\xi=0.480$ nm. Dotted line: Bulk resistivity $\rho_0(T)$ described on the basis of a Bloch-Gruneisen model, using Eq. (4), $\rho_R=15.072$ nΩ m, the constants $A=29.427$ nΩ m, $B=-9.8996\times10^{-4}$; $C=3.3994\times10^{-2}$, and $\theta=172.1$ K. Solid line: film resistivity $\rho(T)$ described on the basis of a Bloch-Gruneisen model using the parameters ρ_R, A, B, C, and θ quoted, and the ratio $\sigma/\sigma_0=\rho_0/\rho$ predicted by mSXW theory.

The issue regarding the size of the corrugations and the scale of distance over which they take place can be viewed from a somewhat different perspective. The SXW theory is a perturbation theory, that uses wave functions labeled by a wave vector k_z that is quantized as a consequence of the electrons being confined between two parallel potential barriers. It is assumed that the presence of the rough surface does not alter this description; in this sense the presence of the rough surface is considered a perturbation. However, the upper and lower surfaces of the metallic film are certainly *not* parallel to each other; this is well illustrated by the amplitude $\delta=11.7$ nm of the ACF measured in the scale of 600 nm$\times$600 nm. The question naturally arises: How rough can the surface be before the effect of the roughness can no longer be considered a perturbation and the mSXW formalism breaks down? As discussed in Ref. 11, the answer is: subbands with well-defined labels $q_n=n\pi/t$ will be observable as long as the rms height fluctuation $\zeta(L_0)$ would satisfy $\zeta(L_0)\leqslant\lambda_F$, where

$$\zeta(L_0)=\sqrt{\langle[h(x,y)-\langle h(L_0)\rangle]^2},$$

$h(x,y)$ represents the height measured at position (x,y), the symbol $\langle\rangle$ denotes an average over an area $L_0\times L_0$, $L_0=2(td)^{1/2}$, where d is the lattice constant, t the film thickness, and λ_F denotes the relevant scale of distance in the problem, the Fermi wavelength. The lattice constant measured via x-ray diffraction, is $d=0.235$ nm; therefore $L_0=8.1$ nm.

We evaluated $\zeta(L)$ for the 20 images used to compute the ACF shown in Fig. 3(a) selecting for each image a submatrix of 128$\times$128 pixels corresponding to $L=10$ nm. The average of $\zeta(L)$ over the twenty 10 nm$\times$10 nm images is 0.45 nm, indicating that the film has a smooth texture over distances of the order of 10 nm. Within the 20 images we found 2 for which $\zeta(L)>1$ nm; these correspond to steep valleys that are remnants of grain boundaries. These valleys are separated by large distances D of the order of several hundred nm [Fig. 1(c) from Ref. 15], the typical lateral dimensions of the crystalites that coalesced to form the film. If the 2 images for which $\zeta(L)>1$ nm are deleted, the average of $\zeta(L)$ over the remaining 18 images is 0.35 nm.

These figures illustrate that in spite of the fact that the 70 nm thick gold film is rough over distances that are long when compared to $L=10$ nm, the film exhibits a surface that is smooth (to within one electron wavelength) over distances $L\leqslant10$ nm, except perhaps near valleys that are the remnants of grain boundaries. Consequently, the perturbative approach of mSXW theory retains its validity.[11]

C. Angular dependence of the reflectivity

One of the new results reported in Sec. IV C that requires an explanation, is a surface reflectivity that approaches zero for a certain angle. This may be understood in terms of the white-noise model used by SXW. If Q_0 is the momentum-independent self-energy of the electron gas in the lowest order within the white-noise approximation, then the reflectivity is given by $R[f,\cos(\theta)]=\{[1-f\cos(\theta)]/[1+f\cos(\theta)]\}^2$.[10] If the surface profile is such that $f>1$, then the reflectivity will approach zero for an angle given approximately by $\cos(\theta_0)=1/f$. The dimensionless parameter $f=k_FQ_0$ is proportional to the ''strength'' of the delta function describing the ACF in (x,y) space—the constant that multiplies the delta function. In practice, f is determined by how deep are the valleys and how tall are the hills found in the surface profile. For the film reported here, characterized by the average ACF displayed in Fig. 3(a) described by a Gaussian with $\delta=0.455$ nm and $\xi=0.480$ nm, the reflectivity approaches zero for $\cos(\theta_0)=0.13969$. The corresponding dimensionless parameter is $f_0=1/\cos(\theta_0)=7.16$. The white-noise reflectivity $R[f_0,\cos(\theta)]$ is plotted in Fig. 4(a).

Increasing the scale of distance over which the surface roughness is measured, makes the hills taller and the valleys deeper. This translates into an increasing ''strength'' of the delta function describing the experimental average ACF with increasing scale of distances, as shown in Figs. 3(a)–3(d). Consequently the parameter f increases, and the angle for which the reflectivity approaches zero decreases, until it becomes smaller than the smallest angle allowed by the model of a particle in a box, $\cos\theta_1=\pi/(tk_F)=0.0037$.

D. Electron-surface scattering and bulk resistivity

The measured film resistivity $\rho(T)$, as well as the corresponding bulk resistivity $\rho_0(T)$ calculated by means of the iterative process outlined in Sec. II, are plotted in Fig. 5. The resistivity ρ of this 70-nm gold film increases by roughly a factor of 4 between 4 K and 300 K, and so does the corresponding bulk resistivity ρ_0. However, the resistivity measured on our 70-nm film at 300 K is about 3 times $\rho_I(300)=22.49$ nΩ m, the intrinsic resistivity of gold ρ_I (arising solely from electron-phonon scattering) at 300 K.[13] This in-

dicates that the resistivity of our film is probably limited by impurities, in spite of using gold wire 99.99% pure as the starting material. This is also reflected in the fact that if Eq. (4) is used to describe the temperature dependence of $\rho_0(T)$, then a constant $A=29.427\,\mathrm{n\Omega\,m}$ and a residual resistivity $\rho_R=15.07\,\mathrm{n\Omega\,m}$ are required. This constant A is more than twice the constant $A=12.359\,\mathrm{n\Omega\,m}$ recommended by Matula for crystaline gold,[13] and the residual resistivity $\rho_R=15.07\,\mathrm{n\Omega\,m}$ is almost as large as $\rho_I(300)$. Therefore, the temperature dependence of $\rho_0(T)$ predicted by mSXW theory in our 70-nm film is inconsistent with the Bloch-Gruneisen description of electron-phonon scattering in crystaline gold, and this is probably a consequence of the enhanced resistivity arising from impurities in our film.

Sambles, Elsom, and Jarvis (SEJ) published measurements of the resistivity of films deposited by thermal evaporation of gold on mica, prepared under conditions of evaporation (temperature of the substrate, 280 °C, speed of evaporation, 5 nm/min) which are similar to ours (temperature of the substrate, 300 °C, speed of evaporation, 6 nm/min), except for the fact that SEJ used gold 99.9999% pure.[15] SEJ prepared films in which the lateral dimension D characterizing the crystalites that make up the samples are also in the range of several hundred nm [Fig. 1(c) of Ref. 15]. Some of the SEJ samples also satisfy the condition that D should be about an order of magnitude larger than t to minimize the effect of grain boundary scattering (Sec. 3). SEJ measured the resistivity of the gold films between 2 and 300 K.

At this point it seems appropriate to clarify similarities and differences between the resistivity data of our 70-nm film and the thinner SEJ films; a comparison of the resistivity of our 70-nm film and the SEJ 80-nm film has been published.[12(b)] At room temperature our resistivity data is almost 3 times larger than the intrinsic resistivity $\rho_I(300)=22.49\,\mathrm{n\Omega\,m}$ expected purely from electron-phonon scattering in crystaline gold. This is in contrast to the SEJ resistivity data, which at 300 K is some 20% to 30% larger than $\rho_I(300)$. As already published, a plausible explanation for this discrepancy may be the fact that the purity of our starting material, 99.99%, *is 2 orders of magnitude lower than the purity of 99.9999% used by SEJ.*[12]

Since SEJ samples exhibit a resistivity close to that expected from crystaline gold, and were evaporated using a speed of evaporation and a substrate temperature close to what we used in preparing our 70-nm film, we may wonder what the predictions of mSXW theory would be if the SEJ samples had a surface characterized also by a Gaussian ACF with $\delta=0.455\,\mathrm{nm}$ and $\xi=0.480\,\mathrm{nm}$. To answer this question we proceeded to analyze the data corresponding to the SEJ films and calculated by means of the iterative process outlined in Sec. II, for each of the 4 thinner SEJ films and for each temperature T, the corresponding bulk resistivity $\rho_0(T)$ predicted by mSXW theory using a Gaussian ACF with the parameters δ and ξ measured on our 70 nm film. The interesting result is that for the 4 thinner SEJ films, the temperature dependence of $\rho_0(T)$ predicted by mSXW theory turns out to be consistent with Eq. (4), using the constants A, B, C, and θ recommended by Matula for crystaline gold, but with slightly different residual resistivities ρ_R for each film. We excluded from the analysis SEJ films thicker than 126 nm,

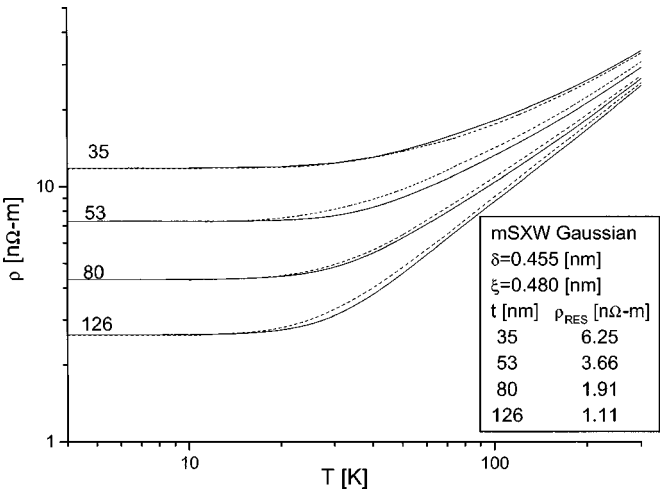

FIG. 6. Dotted line: resistivity of the 35, 53, 80, and 126 nm thick gold films on mica reported in Fig. 3(a) of Ref. 15. Solid line: film resistivity $\rho(T)$ described on the basis of a Bloch-Gruneisen model, using Eq. (4), ρ_R as listed, and the constants $A=12.359\,\mathrm{n\Omega\,m}$, $B=-9.8996\times10^{-4}$; $C=3.3994\times10^{-2}$; $\theta=172.1\,\mathrm{K}$ from Ref. 13, and using the ratio σ/σ_0 predicted by mSXW theory for an ACF described by $f(x,y)=\delta^2\exp[-(x^2+y^2)/\xi^2]$, with $\delta=0.455\,\mathrm{nm}$, $\xi=0.480\,\mathrm{nm}$.

for two reasons: (i) the thickness of these films begins being comparable to the lateral dimension D characterizing the grains, therefore one might expect enhanced grain-boundary scattering in these thicker films; (ii) the thicker films were shown to be polycrystaline when examined by reflection high-energy electron diffraction.[15]

The fact that $\rho_0(T)$ predicted by mSXW theory for the four SEJ films is consistent with what is expected from electron-phonon scattering plus electron-impurity scattering in crystaline gold, means that the resistivity computed from the Bloch-Gruneisen model and from the ratio $\sigma(T)/\sigma_0(T)$ predicted by mSXW theory, should be comparable to the measured film resistivy. This is, indeed, the case: In Fig. 6 we plot the original SEJ data as a dotted line, and the theoretical predictions as a solid line, in the same double logarithmic scale used by SEJ. The predictions are based on a Bloch-Gruneisen model [Eq. (4)] describing electron-phonon scattering in the bulk, corrected for the ratio $\sigma/\sigma_0=\rho_0/\rho$ predicted by mSXW theory [Eq. (2)] describing electron-surface scattering. The interesting result is that the residual resistivity predicted by mSXW theory *turns out to be different for films of different thickness*—despite the fact that the films were evaporated under similar conditions of evaporation—and decrease as the thickness of the film increases; this is at variance with the constant residual resistivity (independent of film thickness) that has been assumed for several decades in the analysis of size-effect data. This might be expected if thicker films had a smaller concentration of impurities than thinner films, something consistent with the fact that at 4 K, the bulk mean free path ℓ predicted by mSXW theory grows larger as the film grows thicker.

It is interesting to note that on these films, which are over 100 atoms thick, the increase in resistivity induced by electron-surface scattering predicted by theory at $T\leqslant10\,\mathrm{K}$, amounts to 17% in our 70-nm film, and roughly 42% to 53% in the SEJ films. It is also interesting to note that the resis-

tivity ratio $RR=\rho_0(300)/\rho_0(4.2\,K)$ predicted by theory, is 4.57 in our 70-nm film, and it is 4.50, 7.52, 13.1, and 21.9 in the SEJ-35, SEJ-53, SEJ-80, and SEJ-126-nm films, respectively.

As shown in Fig. 6, we have reproduced approximately (to within 7% or better) the temperature dependence and the thickness dependence of the resistivity of these four SEJ films between 4 and 300 K, using mSXW theory and a Gaussian ACF characterized by $\delta=0.455\,nm$ and $\xi=0.480\,nm$, *without using any adjustable parameter*. There is an interesting corollary to this unexpected result: If the surface of the SEJ films were described by a Gaussian characterized by the same parameters (δ, ξ) we measured on our film, then grain-boundary scattering would contribute very little to the resistivity of the four SEJ films we have analyzed, since the data seems approximately represented by mSXW theory describing electron-surface scattering combined with a Bloch-Gruneisen model that describes electron-phonon scattering in the bulk, *and neither of these models include grain-boundary scattering*.

E. Comparison between the mSXW theory and other theories

At this point it seems appropriate to compare the predictions of the mSXW theory with those based on various other models that have appeared in the literature.

1. Fuchs-Sondheimer model

The first and by far the most popular model used for many decades, is the FS model. Since in the FS theory, R is an adjustable parameter that is assumed to be independent of the momentum of the electron, and in the mSXW theory R depends on the angle θ between the momentum of the incoming electron and the normal to the surface, the question arises regarding which constant R should be used in the classical theory, to compare the FS model with the mSXW model. One natural way to perform such a comparison is to choose the average of the quantum reflectivity $R=\langle R(\theta)\rangle$ predicted by theory. For the film 70 nm thick, the mSXW theory predicts $\langle R(\theta)\rangle=0.479$ in the case of a Gaussian ACF. According to a comparison between the FS theory and the mSXW theory already published,[11] the FS model overestimates the effect of electron-surface scattering by an amount that increases with increasing mean-free-path, due to the fact that the angular dependence of the reflectivity R is completely ignored in the FS model.

At temperatures between 4 and 10 K, the bulk mean-free-path l predicted by mSXW in our 70-nm film is about 55 nm, and it is 134 nm in the SEJ-35, 229 nm in the SEJ-53, 437 nm in the SEJ-80, and 757 nm in the SEJ-126 film, respectively. At temperatures below 10 K, the predictions of the FS model coincide (within 1%) with the predictions of the mSXW model in our sample, because $l/t<1$, but FS overestimates the effect of electron-surface scattering in the SEJ films by an amount around 12%, because in these films $l/t>1$.

2. Soffer's model

Another model that has been used to analyze size effect data is a model proposed by Soffer.[19] Soffer assumes that the motion of the electrons within the metal film is correctly described by a BTE, and introduces the effect of surface roughness via boundary conditions similar to those used in the FS model, except that Soffer's reflectivity R_S is assumed to depend on θ:

$$R_S(\theta)=\exp\left[-\left(\frac{4\pi\delta}{\lambda_F}\cos(\theta)\right)^2\right], \tag{5}$$

where λ_F is the Fermi wavelength and δ is the rms amplitude of the surface roughness. A modification of this model to include grain-boundary scattering was used by SEJ to analyze their data. Fitting the temperature and the thickness dependence of the data measured on six films between 2 and 300 K, using a model containing five adjustable parameters, SEJ arrive at the conclusion that $r=\delta/\lambda_F\approx 0.05$, and consequently $\delta\approx 0.026\,nm$, about one-tenth of an atomic diameter. The value of δ measured with the STM on our 70-nm film is about 17 times larger. For $\delta=0.455\,nm$, Soffer's reflectivity [plotted in Fig. 4(a)] leads to an average reflectivity $\langle R_S(\theta)\rangle\approx 0.079$, and hence to predominantly diffuse scattering. If Soffer's theory is to agree with the data for $\delta=0.455\,nm$, then the resistivity measured on the SEJ films should have been about one order of magnitude larger than observed.

Data recorded on samples measured with the STM during the preparatory experiments, indicate that in a continuous film prepared by thermal evaporation of gold on mica, the roughness measured on a nanometric scale is characterized by a rms amplitude δ that is comparable to the Fermi wavelength λ_F. This implies that Soffer's model leads to essentially diffuse scattering in these films.

3. Elsom and Sambles's model

Elsom and Sambles (ES) published a model to account for the effect of the macroscopic surface roughness on the conductivity of thin metal films.[20] ES calculated numerically the conductance of a two-dimensional rectangular grid of conductances whose values are derived from a thickness model. The thickness model used to approximate the structure of the metal film, consists of a random distribution of partially overlapping chopped cones, with the cone height and base radii chosen to have a Gaussian spread about some mean values. Local surface roughness is accounted for by using Soffer's theory, to convert the grid of thicknesses into the corresponding conductances. This demanded the introduction of an effective bulk mean-free-path, which was used to scale the dimensions of the model to the real film. The principal variables involved in this model, are the mean cone base radius, the cone angle and the chopping fraction of the cones.

This model describes the *thickness dependence of the resistivity of metal films that are grown nonepitaxially, which are in their initial stage of growth*. At this stage the film is a structure formed by islands that are beginning to conduct, and where grain-boundary scattering plays a central role, once the islands begin to merge with increasing film thickness. Consequently, in the ES model the resistivity of the film is almost certainly dominated by grain-boundary scatter-

ing and perhaps by percolation through the islands. By contrast, in the mSXW model the film is assumed to be a *continuous epitaxial film*, and the mSXW theory describes the resistivity of the epitaxial film that exhibits a contribution due to surface scattering, with the contribution dominated by electron-surface scattering at the upper and lower surfaces of the film. Thus *the ES model applies to a charge transport regime, which is the opposite of that described by the mSXW model*.

F. Conclusion

This paper departs from the traditional method of analyzing size-effect data. On the one hand, we have used a quantum formulation in which the reflectivity R of the surface is entirely determined by $Q[t,\delta,\xi,\cos(\theta)]$ via Eq. (1), where the function $Q[t,\delta,\xi,\cos(\theta)]$ represents the dissipative part of the self-energy of the electron gas due to electron-surface scattering. Rather than assuming a constant R (e.g., R independent of θ, and the same for films of different thickness), we have used a reflectivity that not only depends on θ, but depends as well on the thickness t, and on the parameters δ and ξ characterizing the roughness of the film. We replaced the strong assumption that R is the same in our 70-nm film and in the SEJ films, by the weak assumption that, because our film and the SEJ films were prepared—with the exception of the purity of the starting material—under similar conditions of evaporation, then the parameters δ and ξ should be about the same. Impurities in the range of 1 part in 10^4 or 1 part in 10^6 should have little incidence in the surface roughness measured with the STM, for impurities distributed at random in such a small concentration may affect the observed resistivity of the film but are not expected to modify its roughness profile, for the images recorded with the STM do not depend on the particular resistance of the sample, as long as it is a conductor.

On the other hand, rather than assuming that the bulk resistivity ρ_0—the resistivity that would be observed in the absence of surface scattering—is the same for films of different thickness prepared on different evaporation runs under similar conditions of evaporation, we *calculated* ρ_0 using the mSXW model and our surface roughness data, and found that ρ_0 predicted by theory consists of two contributions: (a) the intrinsic temperature-dependent resistivity $\rho_I(T)$ arising from electron-phonon scattering, which (if not masked by impurities) is the same for films of different thickness and coincides with the Bloch-Gruneisen model in crystalline gold; and (b) a temperature-independent residual resistivity ρ_R that changes from film to film, even though the films were evaporated under similar conditions. A consequence of this finding is that the resistivity ratio RR predicted by theory changes by almost one order of magnitude from the SEJ-35 film to the SEJ-126 film.

The fact that the rms surface roughness measured on our 70 nm film turns out to be *17 times larger* than the value inferred by SEJ from fitting the temperature and the thickness dependence of the resistivity measured on a family of gold films of different thickness, *using a model containing five adjustable parameters*, casts doubts on the validity of both the theoretical model used in fitting the resistivity data (Soffer's reflectivity and the central role assigned to grain-boundary scattering in the SEJ films), as well as on the underlying assumptions that constitute the basis for the parameter fitting of resistivity data that has dominated the literature for several decades. The discrepancy of nearly a factor of 20 between the measured and the inferred δ reported here casts doubts on the validity of data analysis performed by fitting parameters describing the surface roughness to a set of resistivity data, unless the fitted parameters agree, at least approximately, with the roughness of the films *measured in an independent experiment*. This discrepancy underlines the need of revisiting transport measurements on thin metallic films, and the need of cross-checking the parameters characterizing the surface roughness obtained by fitting transport data, with direct measurements of the surface roughness of the films performed on a nanometric scale with a scanning probe microscope capable of atomic resolution.

To our knowledge, this is the first paper in which the temperature dependence and the thickness dependence of the resistivity predicted by a theory, that uses as input the information contained in the surface roughness measured on a nanometric scale in an independent experiment, agrees approximately with the resistivity measured on a set of thin metallic films. *The theory contains no adjustable parameters*. However, since *the roughness and the resistivity were measured on different films* prepared under similar conditions of evaporation—except for the purity of the starting material—the analysis presented might be considered as evidence supporting the mSXW theory, but certainly may not be considered a proof of its validity until the surface roughness and resistivity are measured *on the same film* on various samples of different thickness.

The results presented cast doubts on the validity of data analysis performed by fitting parameters describing the surface roughness to a set of resistivity data without directly measuring these parameters in an independent experiment. This paper cast doubts on two of the central assumptions that have been used for decades to analyze size-effect data on families of films prepared under similar conditions of evaporation: The assumption that the reflectivity R is a constant independent of the momentum of the electron and is common to all members of the family, and the assumption that the bulk resistivity ρ_0 is common to all members of the family.

VI. SUMMARY

This paper reports on the application of a modified version of the theory of Xeng, Xing, and Wang (mSXW)[11] and illustrates how measurements of the roughness of the surface of a metallic film can be used to calculate the resistivity of the film attributable to electron-surface scattering from first principles, *without free parameters*. We report measurements of the resistivity $\rho(T)$ of a gold film 70 nm thick deposited on mica preheated to 300 °C in UHV, performed between 4 and 300 K, and measurements of the surface topography of the same film performed with a STM. From the roughness measured with the STM we determine the parameters δ (rms amplitude) and ξ (lateral correlation length) corresponding to a Gaussian representation of the average ACF data. We use the parameters δ and ξ determined via STM measurements to

calculate the quantum reflectivity R, and the increase in resistivity induced by electron-surface scattering on this film, according to mSXW theory.

The results indicate that the mSXW theory is able to select the appropriate scale of distance over which corrugations take place, leading to $R \approx 1$ for corrugations taking place over scale of distances that are long when compared to a few λ_F, and $R < 1$ for corrugations taking place over scale of distances that are comparable to λ_F (to within an order of magnitude). The reflectivity R determined by corrugations occurring over a scale of distances comparable to λ_F is such that it approaches zero for a certain angle.

With the parameters δ and ξ measured on our 70 nm thick film, we reproduced approximately (to within 7% or better) the thickness and temperature dependence of the resistivity (between 4 and 300 K) of several gold films on mica reported by Sambles, Elsom, and Jarvis.[15]

The results presented underline the need of revisiting transport measurements on thin metallic films, and the need of cross-checking the parameters characterizing the surface roughness—obtained by fitting transport data—with direct measurements of the surface roughness of the film performed with a scanning probe microscope capable of atomic resolution. This paper casts doubts on two of the central assumptions that have been used for decades to analyze size-effect data on families of metal films of different thickness prepared under similar conditions of evaporation: The assumption that the reflectivity R is a constant independent of the momentum of the electron and the same for films of different thickness, and the assumption that the bulk resistivity ρ_0 is common to all members of the family. The results of this paper suggest that the relevant quantities controlling electron-surface scattering in continuous gold films of arbitrary thickness, are the parameters δ and ξ describing the average ACF that characterizes the surface of the sample on a nanoscopic scale, in agreement with the accepted view regarding the conductivity of ultrathin films.

ACKNOWLEDGMENTS

R.M., G.K., and L.M. gratefully acknowledge funding by FONDECYT under Contract No. 1960914, by Fundacion ANDES under Contract No. C-12776, by FONDAP under Contract No. 11980002, and by Universidad de Chile under Contract No. EDID99/008. P.H. gratefully acknowledges funding by FONDECYT under Contract No. 1990304.

*Corresponding author: Departamento de Física, Facultad de Ciencias Físicas y Matemáticas, Universidad de Chile, Blanco Encalada 2008, Casilla 487-3, Santiago, Chile. Email address: RAMUNOZ@TAMARUGO.CEC.UCHILE.CL FAX: 56-2-696-7359.

[1] J. M. Ziman, *Electrons and Phonons* (Clarendon Oxford, 1960).
[2] D. Schumacher, Thin Solid Films **152**, 499 (1987).
[3] E. H. Sondheimer, Adv. Phys. **1**, 1 (1952).
[4] Z. Tesanovic *et al.*, Phys. Rev. Lett. **57**, 2760 (1986).
[5] N. Trivedi and N. W. Aschroft, Phys. Rev. B **38**, 12 298 (1988).
[6] K. M. Leung, Phys. Rev. B **30**, 647 (1984).
[7] C. S. Chu and R. S. Sorbello, Phys. Rev. B **38**, 7260 (1988).
[8] G. Fishman and D. Calecki, Phys. Rev. Lett. **62**, 1302 (1989).
[9] J. C. Hensel *et al.*, Phys. Rev. Lett. **54**, 1840 (1985).
[10] L. Sheng, D. Y. Xing, and Z. D. Wang, Phys. Rev. B **51**, 7325 (1995).
[11] R. C. Munoz *et al.*, J. Phys.: Condens. Matter **11**, L299 (1999).
[12] (a) R. C. Munoz *et al.*, Phys. Rev. B **61**, 4514 (2000); (b) R. C. Munoz *et al.*, J. Phys.: Condens. Matter **12**, 2903 (2000).
[13] R. A. Matula, J. Phys. Chem. Ref. Data **8**, 1147 (1979).
[14] D. Schumacher, *Surface Scattering Experiments with Conduction Electrons* (Springer-Verlag, Berlin, 1993).
[15] J. R. Sambles, K. C. Elsom, and D. J. Jarvis, Philos. Trans. R. Soc. London, Ser. A **304**, 365 (1982).
[16] D. Porath, Y. Goldstein, A. Grayevsky, and O. Millo, Surf. Sci. **321**, 81 (1994).
[17] D. Calecki and G. Fishman, Surf. Sci. **229**, 110 (1990).
[18] G. Fishman and D. Calecki, Phys. Rev. B **43**, 11 581 (1991).
[19] S. B. Soffer, J. Appl. Phys. **38**, 1710 (1967).
[20] K. C. Elsom and J. R. Sambles, J. Phys. F: Met. Phys. **11**, 647 (1981).